PHYSICAL REVIEW E **81**, 035301(R) (2010)

Turbulent spot evolution in spatially invariant boundary layers

Jens H. M. Fransson
Linné Flow Centre, KTH Mechanics, SE-10044 Stockholm, Sweden
(Received 7 January 2010; published 9 March 2010)

A demanding task, for successful fluid dynamic design in many industrial applications, is being able to predict the transition to turbulence location in boundary layer flows. The focus of the present experimental study is on the late stage of transition scenarios where turbulent spots are borne. We report on a natural stabilizing mechanism on the growth rate of turbulent spots, which takes place in a specific bypass transition scenario, and show that there is a palpable history effect of the origin of the turbulent spot on the streamwise evolution. Furthermore, experimental evidence on Reynolds number effects on the spot evolution in boundary layers is put forward. This has been made possible by setting up an idealized experiment, which usually only is considered as a schoolbook example.

DOI: 10.1103/PhysRevE.81.035301 PACS number(s): 47.27.Cn, 47.20.Pc, 47.27.nb

Today, it is well known that a boundary layer (BL) flow can transition to turbulence via different routes depending on surrounding parameters, such as surface roughness, free stream turbulence (FST), and background acoustic noise [1]. There are two theories describing the primary disturbance growth: one is based on a modal representation of perturbations [2], while the other is a nonmodal approach [3] of the linearized perturbation equations. The former, with exponentially growing disturbances, describes well flows with low background disturbance levels typically encountered in free flight and hydraulically smooth surfaces. The latter, with algebraically growing disturbances, describes satisfactory different types of bypass transition scenarios [4] such as in flows with FST or surface roughness. FST is known to induce unsteady elongated streamwise streaks of alternating low- and high-speed fluid [5] typically encountered in turbomachinery flows where the flow approaching the turbine blades is often highly disturbed. The energy of these streaky structures grows algebraically and their spanwise size depends both on the FST intensity, defined as the streamwise root-mean-square velocity u_{rms} over the free stream velocity U_∞, and the characteristic length scales in the FST. The common feature of these two very different transition scenarios occurs when the primary instability reaches a certain amplitude and breaks down to turbulence, probably through a secondary instability mechanism [6], which locally gives birth to turbulent spots. Turbulent spots and their streamwise evolution play a major role in the late stage of most transition scenarios [4]. The appearance of turbulent spots in laminar BLs was first noted by Emmons [7], who proposed a turbulent spot probability appearance model, which lately has proven to work fairly well for the FST-induced transition scenario [8]. Studies of turbulent spots in all canonical shear flows have been reported extensively in the past, but there are still some open questions in BLs, which partly are the focus of this Rapid Communication. Flow visualizations in a growing zero-pressure-gradient boundary layer show that the turbulent spot takes the shape of an arrowhead with its tip pointing downstream [9]. The half-width spanwise spreading angle (α) of the spot was concluded to be around 10° and independent of Reynolds number (Re) [10], and the breakdown of oblique waves at the trailing corners of the spot is believed to be part of the rapid growth in the spanwise direction [11]. However, over the past years α angles in the range $6°-12°$ have been reported and Re dependence has been brought up as a physical explanation [12]. Except for a direct numerical simulation of turbulent spots in the asymptotic suction boundary layer (ASBL) [13] (from here on denoted DNS) no clear evidence of Re effects has been put forward. The effect of favorable pressure gradient has been shown to damp the spreading of the spot with 50% both in the spanwise and in the wall-normal direction and the shape becomes triangular with rounded edges [14]. The explanation for the reduced growth was attributed to the fuller shape of the mean velocity profile, which leads to a more stable BL and in turn will not allow for tip waves to grow. A compilation of reported leading and trailing edge speeds of turbulent spots suggests that a smaller α angle makes the spot propagate faster; typical values are around 0.9 and 0.5 of U_∞, respectively.

In the present experimental study the effects of initial condition, Re, and FST on turbulent spot evolution have been studied while keeping the BL thickness constant. This type of study can only be performed in the ASBL, where continuous suction through the wall gives rise to a BL, which does not grow in space, i.e., a spatially invariant BL. The wall-normal streamwise velocity profile $u(y)$ in the ASBL can readily be derived from the Navier-Stokes and the continuity equations as

$$u(y) = U_\infty\{1 - e^{yV_{\mathrm{w}}/\nu}\}, \tag{1}$$

where V_{w} and ν are the suction velocity (<0) and the kinematic viscosity, respectively [15]. With the access of an analytical solution [Eq. (1)] it is straightforward to calculate the displacement and the momentum thicknesses which become $\delta_1 = -\nu/V_{\mathrm{w}}$ and $\delta_2 = \delta_1/2$, respectively, giving a constant shape factor, $H_{12} = \delta_1/\delta_2 = 2$, independent of the suction velocity. The Reynolds number based on the displacement thickness, thus, becomes $\mathrm{Re} = -U_\infty/V_{\mathrm{w}}$ allowing for Re changes without necessarily changing the BL thickness. The present experiments were carried out over a 5.7-m-long flat aluminum plate, mounted horizontally in the minimum-turbulence-level wind tunnel at The Royal Institute of Technology. The plate is followed by a trailing edge flap for leading edge stagnation line adjustment [see Fig. 1(a)]. A porous

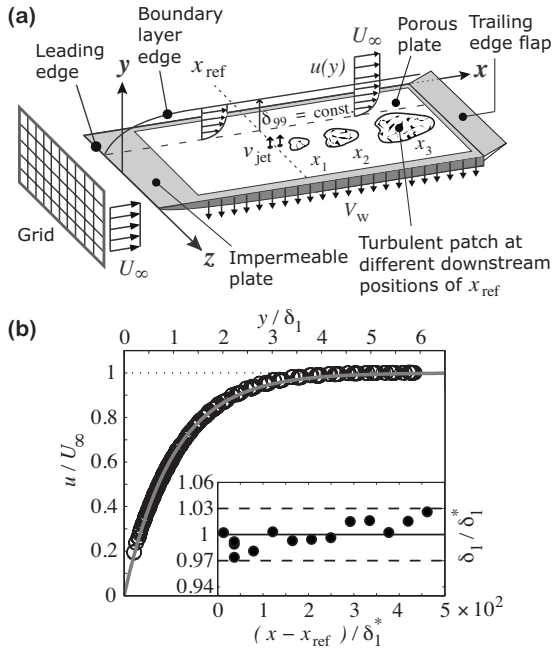

FIG. 1. (a) Schematic of the flow field over a flat plate subjected to constant suction. Note that this sketch is not according to scale. (b) 13 mean streamwise velocity profiles at the streamwise positions indicated in the inset, where the displacement thickness (by direct integration) of each profile is shown. δ_1^* is the averaged δ_1 in the streamwise extent. Solid gray line corresponds to the theoretical ASBL profile [Eq. (1)].

plate (2.25×1 m^2) made of a sintered plastic material, with an averaged pore size of 16 μm, was inserted into the aluminum plate at 0.36 m from the asymmetric leading edge [16] allowing for continuous suction to be applied through the surface. Interested readers are referred to [17], where a similar setup was used. Turbulent spots were generated at the reference position, $x_{ref}=1.85$ m from the leading edge, by means of short pulsed wall jets through one or two streamwise located holes in the porous plate. The ceiling was adjusted for zero-pressure gradient with a wall suction velocity corresponding to a displacement thickness of $\delta_1=1.45\pm0.04$ mm over a streamwise distance of $(x-x_{ref})/\delta_1=13-454$. This is shown in the inset of Fig. 1(b). The wall-jet pulse was computer generated through a digital-to-analog signal board to an audio amplifier driving a sealed loud speaker, which was connected to the hole(s) through vinyl hosing. The pulse height of the signal to the loud speaker was quantified by measuring the dc output voltage (VDC) from the amplifier with a voltage meter. The measurements were performed with hot-wire anemometry triggered by the pulse with a suitable time delay (t^*), and the probe was traversed in the spanwise direction (91 positions), at $y=\delta_1$, in the wall-normal direction (30 positions), at the midplane $z=0$, and in the streamwise direction (six positions), $(x-x_{ref})/\delta_1=(102, 135, 169, 202, 235, 269)$. At each position the turbulent spot measurement was repeated 80 times giving a total number of over 400 000 generated spots considering all experiments performed. The effects of initial condition and FST were investigated by changing the jet strength, the pulse duration, and the number of holes (one vs two) and by applying two different turbulence-generating grids, respectively. All the experimental cases are summarized in Table I.

Figure 2 shows the shape of the turbulent spot, both in terms of mean velocity access and deficit in Figs. 2(a) and 2(b), and the turbulence intensity in Figs. 2(c) and 2(d). One may conclude that there is a region of velocity deficit at the leading edge of the spot sitting on top of a larger near wall region of velocity access [Fig. 2(a)]. On the flanks of the turbulent spot, seen from above, velocity deficit regions exist both at the leading edge of the spot and around the midregion [Fig. 2(b)]. The maximum turbulence intensity is greater than 15% in all cases and the distribution [Figs. 2(c) and 2(d)] shows that the region of velocity access in the trailing edge of the spot [Figs. 2(a) and 2(c)] is a calm region with a relatively low fluctuation level. The turbulence intensity distribution seen from above [Fig. 2(d)] has a triangular shape with rounded edges, i.e., similar to what has previously been reported for turbulent spots with favorable pressure gradient.

The leading and trailing edge propagation speeds as well as the α angle of the turbulent spot were determined in a systematic way, which is shown in Fig. 3 for a specific case. A rectangle was drawn around the velocity derivate contour line, corresponding to a particular value, for each downstream location as illustrated in Fig. 3(a). The tx and zx diagrams were drawn [Fig. 3(b)] and the leading and trailing edge propagation speeds as well as the α angle of the turbulent spot could be determined. This procedure was repeated for all the experimental cases listed in Table I. In Fig. 3(b) two half-width spreading angles are exposed where the first

TABLE I. Experimental parameters. At x_{ref}, grid$_1$ and grid$_2$ give rise to a maximum streak amplitude inside the BL of 4.4% and 1.3%, respectively. Figures are rounded.

Case	No. holes	VDC	Pulse (ms)	δ_1 (mm)	U_∞ (m/s)	Re	FST	Scans
EXP1	1	12	6	1.45	5	500		xy, xz
EXP2	2	12	6	1.45	5	500		xy, xz
EXP3	2	12	120	1.45	5	500		xy, xz
EXP4	2	12	6	1.45	6	600		xy, xz
EXP5	2	12	6	1.45	4	400		xy, xz
EXP6	2	12	6	1.45	5	500	grid$_1$	xy, xz
EXP7	2	12	6	1.45	5	500	grid$_2$	xy, xz

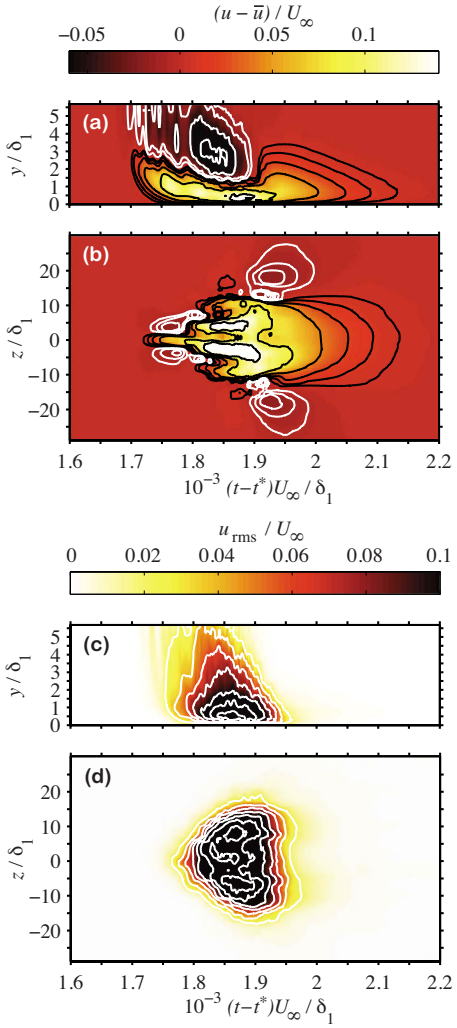

FIG. 2. (Color online) Turbulent spot at $(x-x_{ref})/\delta_1=269$, which travels from right to left (case EXP2). (a) and (b) show contour plots of positive (yellow/bright) and negative (black/dark) perturbations in the xy (center line) and xz planes ($y=\delta_1$), respectively. Black and white contour lines correspond to the values (0.005, 0.01, 0.02, 0.04, 0.08, 0.13) and (−0.08, −0.05, −0.02, −0.009), respectively. (c) and (d) show the corresponding contour plots of u_{rms}/U_∞. White contour lines correspond to the values (0.02:0.02:0.14).

one is attributed to an initially linear spreading development of the localized disturbance, while the second is the angle of interest corresponding to the spreading angle of the fully developed turbulent spot.

Previous investigators have claimed that the evolution of turbulent spots in BLs is Re independent (except for [13]) and that all fully developed turbulent spots propagate with the same characteristics independent of their origin, i.e., there is no history effect regarding the initial condition. In Figs. 4(a) and 4(b) the leading and trailing edge propagation speeds and the α angle are plotted, respectively, for EXP1–EXP5. Neither experiments nor DNS shows a notable change in the leading edge propagation speed of the turbulent spot for increasing Re. However, the DNS shows a significant decrease in the trailing edge speed with Re, while the experiments does not. This discrepancy can be attributed to the

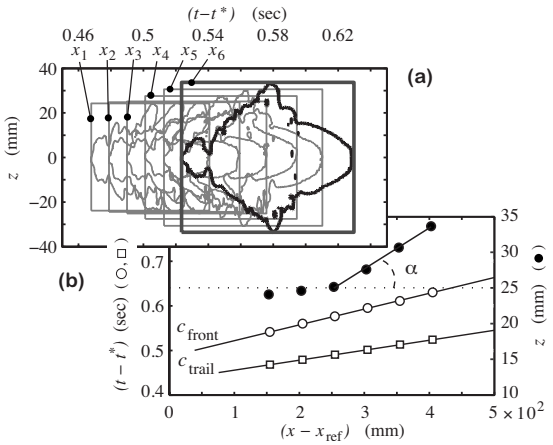

FIG. 3. Case EXP3. (a) Dimensionless contour lines of the velocity trace derivative, $(du/dt)\delta_1/U_{local}^2=0.001$, in the xzt plane at $y=\delta_1$ for the six streamwise positions. (b) tx and zx diagrams extracted from the rectangles enclosing each contour line in (a). Propagating frontal and trailing edge turbulent spot speeds are then calculated as $dx/dt=c_{front}=0.895U_\infty$ and $c_{trail}=0.567U_\infty$ in a least-squares fit sense to the (○) and (□) symbols, respectively. Half-spreading angle becomes $\alpha=3.3°$ determined in a least-squares fit sense to the (●) symbols.

initial condition. It is clear from Fig. 4(b) that the shape of the localized disturbance has a large impact on the spreading. EXP2 is the reference case using the two holes in the plate and was generated with a short pulse, EXP1 uses one single hole, and EXP3 was generated with a long pulse; all cases have the same amplitude (see Table I). Note that EXP2 vs EXP3 gives a 60% reduction in the spreading. It should be pointed out that no effort was made in trying to simulate the

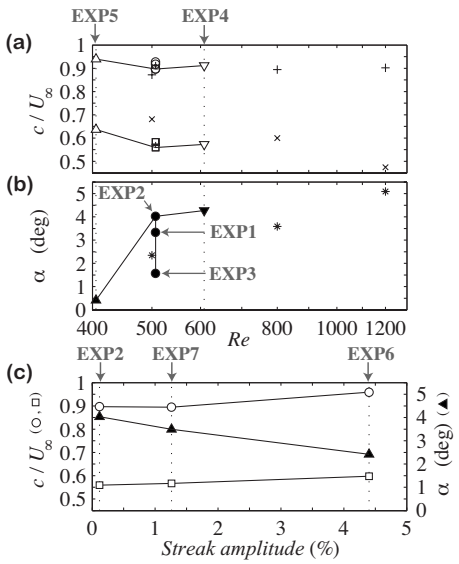

FIG. 4. (a) Initial condition and Re dependence on turbulent spot propagation speed and (b) the half-width spreading angle (α). (c) Streak amplitude dependence on turbulent spot propagation speed and the α angle. Open and filled symbols correspond to propagation speeds and half-width spreading angles, respectively. The experimental case (Table I) is indicated with an arrow to the symbols. DNS results [13] are shown with (+,×,*) symbols.

same localized disturbance as in the DNS, but from the results it is clear that if a match of the results, between experiments and DNS, is sought after the same localized disturbance has to be analyzed. Here, we are satisfied with the proof that the shape of the localized disturbance is important for the turbulent spot characteristics at least for the Re considered.

It can be argued that for increasing Re the α angle will level off to a constant value, which for a zero-pressure-gradient boundary layer probably would be around $10°-12°$ and hence independent of Re once a threshold Re has been reached. The reason for this saturation would be the presence of tip-wave breakdown, which needs a certain amount of velocity deficit on the flanks of the spot and a matching Re to cause exponential growth of oblique tip waves. Even though the critical Re for the onset of Tollmien-Schlichting waves in the ASBL is on the order of 10^4 the spot may modulate the BL shape in the velocity deficit regions in such extent that it will become susceptible to exponential growth of oblique waves and in turn level off the α angle due to the fact of being a stronger mechanism than the Re effect.

Westin *et al.* [18] showed that Tollmien-Schlichting waves grow less when the BL is subjected to FST but no physical explanation was given. Steady streamwise streaks, generated by means of roughness elements, inside the BL have been shown to sensibly delay transition to turbulence [19]. The underlying physical mechanism is attributed to the extra turbulence production term due to the spanwise modulation of the BL. The contribution from $-\langle uw\rangle \partial U/\partial z$ turns out to be of negative sign [20] and together with the viscous dissipation it can overcome the wall-normal production term, $-\langle uv\rangle$, acting on $\partial U/\partial y$. In Fig. 4(c) one may observe that for increasing FST intensity, or equivalently increasing streak amplitude, the growth of the turbulent spot in the spanwise direction is diminished. The reduction for this moderate level of FST intensity is as much as 40%. This means that the bypass transition scenario of FST has an inherent stabilizing mechanism due to the presence of streamwise streaks. It has previously been observed [8] that for increasing FST intensity the relative length of the transitional zone increases, but no physical interpretation was attempted. This piece of finding is important in any development of reliable transition prediction models that can be used in present computational fluid dynamics programs as an engineering tool. Noteworthy is that the leading edge propagation speed becomes as high as $0.96U_\infty$ with the presence of FST, which appears to facilitate the spreading when the spot breaks new ground.

In this Rapid Communication we report on three momentous results (1)–(3) on the turbulent spot evolution in BL flows. These findings are the result of studying turbulent spot evolution in the so-called asymptotic suction boundary layer where the boundary layer thickness and the Re are decoupled from each other. (1) Experimentally a clear Re dependence on the development of a turbulent spot in a BL flow is being reported. (2) We show that there is a palpable history effect of the origin of the turbulent spot. Results (1) and (2) explain the large variety of turbulent spot spreading angles reported over the years in zero-pressure-gradient boundary layers. (3) Unsteady streamwise elongated streaks appearing naturally in a FST transitional boundary layer has a damping effect on the development of turbulent spots, and consequently the relative length of the transitional zone increases with increasing streak amplitude or equivalently with increasing FST intensity.

The Göran Gustafsson Foundation is greatly acknowledged for their financial support.

[1] Y. S. Kachanov, Annu. Rev. Fluid Mech. **26**, 411 (1994).
[2] G. B. Schubauer and H. K. Skramstad, J. Aeronaut. Sci. **14**, 69 (1947).
[3] L. N. Trefethen, A. E. Trefethen, S. C. Reddy, and T. A. Driscoll, Science **261**, 578 (1993).
[4] M. V. Morkovin, in *Viscous Drag Reduction*, edited by C. S. Wells (Plenum Press, New York, 1969).
[5] M. Matsubara and P. H. Alfredsson, J. Fluid Mech. **430**, 149 (2001).
[6] P. Andersson, L. Brandt, A. Bottaro, and D. S. Henningson, J. Fluid Mech. **428**, 29 (2001).
[7] H. W. Emmons, J. Aeronaut. Sci. **18**, 490 (1951).
[8] J. H. M. Fransson, M. Matsubara, and P. H. Alfredsson, J. Fluid Mech. **527**, 1 (2005).
[9] J. W. Elder, J. Fluid Mech. **9**, 235 (1960).
[10] I. Wygnanski, M. Sokolov, and D. Friedman, J. Fluid Mech. **78**, 785 (1976).
[11] I. Wygnanski, J. H. Haritonidis, and R. E. Kaplan, J. Fluid Mech. **92**, 505 (1979).
[12] B. A. Singer, Phys. Fluids **8**, 509 (1996).
[13] O. Levin and D. S. Henningson, J. Fluid Mech. **584**, 397 (2007).
[14] Y. Katz, A. Seifert, and I. Wygnanski, J. Fluid Mech. **221**, 1 (1990).
[15] A. A. Griffith and F. W. Meredith, Aeronautical Research Council London Technical Report No. 2315, 1936 (unpublished).
[16] J. H. M. Fransson, Exp. Fluids **37**, 929 (2004).
[17] J. H. M. Fransson and P. H. Alfredsson, J. Fluid Mech. **482**, 51 (2003).
[18] K. J. A. Westin, A. V. Boiko, B. G. B. Klingmann, V. V. Kozlov, and P. H. Alfredsson, J. Fluid Mech. **281**, 193 (1994).
[19] J. H. M. Fransson, A. Talamelli, L. Brandt, and C. Cossu, Phys. Rev. Lett. **96**, 064501 (2006).
[20] C. Cossu and L. Brandt, Eur. J. Mech. B/Fluids **23**, 815 (2004).